5-2020

Analyzing the effects of of seasonal land cover and precipitation on the sediment delivery ratio of an agriculture dominated watershed.

Jonah Liebman
University of Louisville

ANALYZING THE EFFECTS OF SEASONAL LAND COVER AND PRECIPITATION ON THE SEDIMENT DELIVERY RATIO OF AN AGRICULTURE DOMINATED WATERSHED

By

Jonah Liebman

B.A., Washington University in St. Louis, 2016

A Thesis

Submitted to the Faculty of the

College of Arts and Sciences of the University of Louisville

in Partial Fulfillment of the Requirements

for the Degree of

Master of Science

in Applied Geography

Department of Geography

University of Louisville

Louisville, Kentucky

May 2020

ANALYZING THE EFFECTS OF SEASONAL LAND COVER AND PRECIPITATION ON THE SEDIMENT DELIVERY RATIO OF AN AGRICULTURE DOMINATED WATERSHED

By

Jonah Neal Liebman

B.A., Washington University in St. Louis

A Thesis Approved on

April 14, 2020

By the following Thesis Committee:

____

Dr. C. Andrew Day

____

Dr. Jafar Hadizadeh

____

Dr. Tamara Sluss

ACKNOWLEDGEMENTS

I would like to give much deserved praise and thanks to Dr. C. Andrew Day for the immense amount of help throughout the thesis process. Without his persistent motivation, perpetual guidance, and time management, the completion of this thesis would have been impossible.

In addition, I would like to thank Dr. Hadizadeh for his guidance throughout the proposal process and offering to be a second department member to read my thesis. With his help, we all were able to devise a path through this semester and carry through with our intended research interests. I would also like to extend thanks to Dr. Tamara Sluss, who has agreed to be a reader on my thesis and has been a great teacher during our time in Sustainability and the Natural Environment course.

Further, I would like to thank my girlfriend and biggest emotional support, Alissa Rost for talking with me through many a stressful night throughout the thesis proposal process. As an ear for listening and a shoulder to lean on, she has helped me make it through the other end of the thesis proposal and writing process with my mind in one piece.

And lastly, tremendous thanks go out to my parents, Drs. Karla Guess and Curt Liebman, for raising me into the person I am, supporting me every step of the way, and instilling in me drive for education and working hard in all I do.

ABSTRACT

ANALYZING THE EFFECTS OF SEASONAL LAND COVER AND PRECIPITATION ON THE SEDIMENT DELIVERY RATIO OF AN AGRICULTURE DOMINATED WATERSHED

Jonah N. Liebman

April 24, 2020

Soil erosion is of escalating importance as increasing population and climate change have put increasing pressures on agricultural food production. Vegetation and precipitation are two factors that control the amount of soil erosion extant within a region. Sediment delivery ratios (SDRs) assess the ratio of soil eroded from a watershed system that is permanently removed from the system through stream sediment discharge. Using 1) river discharge and sediment concentration data and 2) the Revised Universal Soil Loss Equation (RUSLE), this thesis analyzes fluctuations in monthly SDRs for an average hydroclimatological crop-harvest season for the Senachwine Creek watershed, IL. Through calculating average gross soil erosion and sediment yield, it is found that significant fluctuations in watershed soil erosion and sediment yield occur in response to changes in precipitation and crop vegetation cover.

TABLE OF CONTENTS

LIST OF TABLES

LIST OF FIGURES

INTRODUCTION

Soil Erosion

The issue of sediment erosion is of increasing concern globally, especially as population pressures create an increasing demand for food production. With an ever-increasing need for sustainable food resources, a major concern in today's agricultural practices is the incorporation of responsible water resource management practices to reduce soil erosion, one form of soil degradation (Telles, Guimaraes, and Dechen 2011). This is especially important considering that 56% of soil degradation is a result of water erosion (Gruver 2013). Productive lands, defined as land that has produced farm crops within the previous 5 years (Mindat 2019), only account for less than 11% of the Earth's surface and is relied upon to feed the entirety of the world's exponentially increasing population (Blanco and Lal 2010). Therefore, widespread degradation of this limited resource through water erosion has massive impacts on food security, and environmental quality overall.

Though soil erosion is a natural process, it is unfortunately exacerbated by anthropogenic activities, especially as population continues to rise (Adornado, Yoshida, and Apolinares 2009). Natural erosional processes account for approximately 20 gigatons of sediment loss annually (Wilkinson and McElroy 2009) while human activity – in the forms of agriculture, construction, and mining – accounts for more than 100 gigatons of earth material (Hooke 2000), making human activity the dominant agent of geologic change. Because of increasing removal of soil away from the agricultural fields, stream water quality degradation, surface water pollution, and overall watershed degradation can occur (Lamba et al. 2015). Furthermore, with increasing precipitation and temperature fluctuations due to climate change (EPA 2016), there is a predicted increase in soil loss, especially as it relates to the heavily farmed Midwest United States. With increased storm intensity due to more variable climatic conditions, runoff will increase (O'Neal 2005; Easterling and Karl 2001). In one paper detailing 11 case studies conducted in the region, the prediction of increased soil loss ranges from +33% to +274% in 2040 – 2059 relative to 1990 – 1999; and this study even accounts for adaptations of responsible crop management practices forced on by climate change (O'Neal et al. 2005). These predicted increases in soil erosion are significant when considering that as a global average, it takes up to 1000 years for one inch of new topsoil to form (Arsenault 2014).

Conversely, sustainable land management (SLM) practices have been observed to have beneficial effects on reducing erosion (Colman 1954; Griffin and Smith 2001; Morgan and Rickson 2011). SLM includes practices to minimize soil loss in a variety of ways, including practices that prevent land conversion and protect vulnerable areas; prevent and mitigate land degradation and restore degraded soils; control soil erosion; improve soil-water storage; manage soil organic matter for carbon sequestration; manage and enhance soil fertility; promote integrated soil-crop-water management, integrated agroforestry, and agro-silvo-pastoral systems; rehabilitate and sustainably manage dryland environments; improve crop-water productivity; and manage soil salinity in irrigated dryland agriculture (FAO 2019).

Gray and Leiser (1982) summarize the effects of herbaceous vegetation, and to a lesser extent woody vegetation, as it relates to sustainable land management practices in general, and soil erosion mitigation more specifically. For example, foliage and plant residues absorb rainfall energy and prevent soil compaction through interception. In addition, vegetation can physically bind or restrain soil particles while above-ground residues filter sediment out of run-off. Furthermore, above-ground plant residues increase surface roughness, effectively slowing run-off velocity. Plant residues and roots also help maintain soil porosity and permeability, absorbing water and diminishing its eroding properties. Lastly, depletion of soil moisture by plants can delay onset of saturation and runoff (Gray and Leiser 1982).

Conversely, poor land management practices include those which are not sustainable and, instead, lead to land and soil degradation. According to Gabriels and Cornelis (2015), human-induced land degradation incorporates all non-sustainable actions that cause a loss in resilience, defined as the land's ability to recover from external disturbance. The authors break down degradation into three categories: soil degradation, vegetation degradation, and water resources degradation. Considering soil degradation, this form can take place in erosion rates, fertility decline, soil nutrient imbalance, occurrence of soil deficiencies, and salination of soils (Gabriels and Cornelis 2015). One study of erosion and land management practices across the US purports $44 billion per year in financial costs as a result of soil erosion and bad land management practices (Telles, Guimaraes, and Dechen 2011). However, previous studies have even predicted anywhere between $12 - $42 billion in erosion costs due to surface runoff alone (Blanco and Lal 2010).

Sediment Delivery Ratios

To help understand soil loss and the measurement of it in an ecosystem, certain studies have incorporated sediment delivery ratios (SDRs) as representations of erosional effects for a given watershed (Ebrahimzadeh et al. 2018; Fagnano et al. 2012; Lee and Lee 2010; White 2005). A sediment delivery ratio is defined as the stream sediment yield draining from a watershed divided by the gross watershed soil erosion estimated for that same contributing area (NRCS 1998). The resulting ratio assesses the proportion of eroded sediment that is effectively permanently removed from said area through stream discharge. The higher the proportion, the greater the quantity of eroded soil permanently removed from the system in the form of stream sediment – disastrous for sustainable agricultural practices. To clarify, SDRs are commonly used in the field for assessing relationships between gross soil erosion to sediment yield (Ebrahimzadeh et al. 2018; Fagnano et al. 2012; Lee and Lee 2010; White 2005, Evans and Seamon 1997). Drainage area, land use, soil particle size, channel density, topography, and sediment source are all factors that may control SDR values (NRCS 1998). Typical research that incorporates the ratio is used in conjunction with soil loss equations like the Universal Soil Loss Equation (USLE) and the Revised Universal Soil Loss Equation (RUSLE) – both explained in a proceeding section – to estimate soil erosion loss from the catchment before entering the stream system (Ebrahimzadeh et al. 2018; Lee and Lee 2010; Evans and Seamon 1997). Using SDR and the estimated gross erosion from the area (the denominator), suspended sediment yields (numerator) in locations void of in-situ measurement can be calculated. In calculating SDR, several methods have been developed. They usually fall into two methodological groups: areal based formulae and formulae based on in-situ measurements of sediment concentrations and discharge at gaged locations. Regarding the former, Ebrahimzadeh et al. (2018) summarize popular SDR calculations based on areal extent of the watershed. Table 1 provides some example formulae they incorporated (adapted from Ebrahimzadeh et al. 2018).

Areal formula	Source of formula
$SDR_1 = 0.472\ A^{-0.125}$	Vanoni 1975
Log (SDR••$_2$) = 1.8768 – 0.14191 log(25.9A)	Renfro 1975
$SDR_3 = 0.51\ A^{-0.11}$	USDA SCS 1979
$SDR_4 = 0.5656\ A^{-0.11}$	USDA 1972
$\text{Log}(SDR_{5)}) = 1.7935 - 0.14191\ \log(A)$	Renfro 1975
$\text{Log}(SDR_6) = 1.8768 - 0.14191\ \log(10A)$	Maner 1962
$SDR_7 = 0.51\ A^{-0.11}$	USDA 2002
Average SDR = $\sum (SDR_{1\text{-}7}) / 7$	Ebrahimzadeh et. al. 2018

Table 1. Summary of areal equations used by Ebrahimzadeh et al. (2018), where A is watershed area.

Averaging the above equations (bottom row, left column) and applying them on the Nozhian watershed in Western Iran – 335 km^2 in area, gives an SDR of about 26.82%. The authors also found that in using their averaged calculation, the relative error reduced to -1.27%, which is much better than the extremes of -18.99% and 9.10% for other areal methods (Ebrahimzadeh et al. 2018).

With regard to in-situ measurements of sediment concentration and discharge ~~)~~, Lee and Lee (2010) built sediment-rating curves using the relationship between measured suspended sediment concentration and total water discharge for many locations across Southern Korea in order to assess sediment yields in areas lacking in-situ data. After plotting these values of known sediment yields and discharge on a graph, the statistical relationship can be assessed and given as a correlation equation. Once they obtained gross erosion loss estimates for a particular unmeasured location using RUSLE, they enter this discharge data back into the sediment-rating curve to effectively get the proportion of sediment leaving the water basin, and consequently the sediment yield (Lee and Lee 2010).

Another study utilizing sediment-rating curves includes Evans and Seamon (1997). In their paper, they utilize two main data sets in calculating sediment delivery ratios: 1) an extensive hydrologic dataset incorporating discharge and suspended sediment, and 2) established rating curves and discharge-suspended sediment relationships for nine channel cross-sections upstream of Old Woman Creek estuary in Ohio over approximately six months. Noteworthy is that the first dataset uses a gage station upstream of the estuary that only monitors 84% of the overall basin. The authors extrapolated the 6-month dataset to obtain annual values, particularly for annual suspended sediment load, from two cross-sections located up- and downstream of the first dataset's gage location (newly created dataset 3). The SDR was then calculated for the upper 84% of the drainage basin using the RUSLE soil erosion loss estimates and the average annual suspended sediment load extrapolated from dataset 2. Knowing the percent of total average annual stream sediment load – used as a proxy to sediment yield – ~~that is~~ carried by the stream as suspended sediment load, Evans and Seamon were able to calculate the delivery ratio for the watershed, which they assessed to be between 21%-25% (1997). This effectively states that of the total gross soil eroded from the upper 84% of the watershed, around 1/5 to ¼ of the soil is permanently removed from this portion of the watershed (Evans and Seamon 1997).

Sediment yield component

Sediment yield is defined as the amount of sediment reaching or passing a specific point along the stream course over a given period. There are many forms of estimating sediment yields, such as those discussed above (Ebrahimzadeh et al. 2018; Lee and Lee 2010; Evans and Seamon 1997). In addition to estimating this value, extant are many datasets that measure in-situ discharge, suspended sediment concentrations, and resulting sediment yields at hydrologic gage sites ~~across the nation~~. For example, the United States Geologic Survey keeps a variety of information they record at gage sites, including the overall discharge, as well as suspended sediment loads passing the gage at the river's cross-section (USGS 2019a). Multiplying the overall discharge by the sediment concentration gives sediment yield values. In doing so, this data can provide the direct measurements for the suspended sediment yield component of the SDR.

Gross soil loss component

For the total soil erosion component in the SDR equation, models have been created that help estimate and quantify soil loss from a defined area. This calculation incorporates a variety of soil loss components that factor into the resulting mass of soil lost from the surface. Different soil loss equations have been developed to address these components (Wischmeier and Smith 1978, Renard et al. 1997; Aksoy and Kavvas 2005; Kinnel 2010; Benavidez et al. 2018). These models can be broken up into empirical, conceptual, and those based on physical processes (Aksoy and Kavvas 2005; Kinnell 2010).

One important empirical model that has gained popularity and increased application is the Universal Soil Loss equation (Wischmeier and Smith 1978) and its revised version is aptly named Revised Universal Soil Loss Equation (RUSLE) (Renard et al. 1997; Renard et al. 1994). The Universal Soil Loss Equation (USLE) has many variants (Benavidez et al. 2018). The common variables for both the USLE and the RUSLE are as follows: rainfall erosivity (R), soil erodibility (K), slope length (L), slope steepness (S), soil use and management (C), and support practices (P) – acting as a sort of correction factor (de Carvalho et al. 2014). Specific calculations will be discussed in the Data and Methods section. Noteworthy to mention here, the C factor for RUSLE can be calculated intra-annually and is highly dependent on land and vegetation cover (Renard et al. 1994; Renard et al. 1997; Benavidez et al. 2018; Ferreira and Panagopoulos 2014). As a result, intra-annual fluctuation of RUSLE estimates will be highly land- and vegetation-cover-dependent. This characteristic of RUSLE's C-factor and its relationship to vegetation coverage allows for direct assessment of how vegetation coverage can account for erosion estimates over shorter time periods throughout the year (Renard et al. 1994; Renard et al. 1997; Benavidez et al. 2018). In addition, RUSLE includes new rainfall erosivity maps for the United States, changes in soil erodibility due to freeze-thaw and soil moisture, and changes to how topography influences the slope and length factors (Benavidez et al. 2018; Renard et al. 1997).

The RUSLE method has been frequently applied in the past to estimate gross soil loss. For example, Benavidez et al. (2018) explains that USLE and RUSLE were originally developed at the farm plot scale for agricultural land use. This so-called unit plot is defined as one 22.1 m long, 1.83m wide, with an average slope of 9%

(Wischmeier and Smith 1978). In their study, Evans and Seamon (1997) applied RUSLE to show that soil loss values for the watershed at Old Woman Creek, Ohio average 7.26 metric tons/ha/yr for around 5000 polygons of the 69.5km^2 drainage basin based on this unit plot.

While the method was originally created for US farmland, adoption of the RUSLE method globally and on a continental basis has been undertaken using adjusted factor calculations. For example, Naipal et al. (2015) attempted to apply the equation on a global scale with a resolution of 30 arc-seconds by using US and European datasets for calculation of the R factor that incorporate annual precipitation, mean elevation, and a simple precipitation intensity index for different climate classifications. Further, Panagos et al. (2015) constructed rainfall erosivity maps at 1km resolution for the whole of Europe to apply RUSLE to the region. Using a large rainfall dataset, da Silva (2004) constructed a spatially interpolated map of R factors in Brazil to enable RUSLE's application in his home country. In tropical areas such as Southeast Asia, the R-factor by El-Swaify, Gramier, and Lo (1987) was used extensively in Thailand, Sri Lanka, and the Philippines. In arid regions, Arnoldus (1980) derived erosivity equations for Morocco and other locations in West Africa. In the United States specifically, R-factor calculation has even been adopted on a monthly basis as precipitation data across the country is more readily available (Renard et al. 1997).

The K-factor in the RUSLE equation ~~that~~ can be adjusted based on areal application. While the original K-factor was created for medium-textured soils in the Midwestern US with an upper silt fraction less than 70% (Renard et al. 1997), El-Swaify and Dangler (1976) applied the factor to the region of Hawaii specifically. For the

European Union, Panagos et al. (2015) created a soil erodibility raster data set (around 500m resolution) used for validation for different soils across the EU. Noteworthy is that these K-factors must be soil specific, so knowing the soil makeup of an area is crucial for appropriate application (Benavidez et al. 2018).

Further, the combined LS factors undergo calculation modifications when applied to different regions. David (1988) helped modify the LS calculation for areas in the Philippines while Morgan (2005) did the same for Great Britain, which was later adopted for application in parts of India (Nakil and Khire 2016; Sinha and Joshi 2012) and Greece (Rozos et al. 2013). In addition, Desmet and Govers (1996) used DEMs to show its application in a GIS environment over topographically complex terrains when compared to the original method set forth by Wischmeier and Smith (1978).

Lastly, the C-factor has undergone similar adjustments in calculation when applied to difference land coverages across the globe (Benavidez et al. 2018). RUSLE incorporates previous management, canopy cover, surface cover and roughness, and the effects of soil moisture on potential erosion to produce a soil loss ratio, used in the R factor to produce a value for the C factor (Renard et al. 1997). Other studies found unique C-factor values corresponding to different land covers within specific geographic locations: David (1988) for the Philippines, Morgan (2005) for across Europe, Fernandez (2003) for the United States, and Dymond (2010) for New Zealand. In addition, and important for the scope of this thesis, Van der Knijff, Jones, and Montanarella (2000) and Ma, Wang, and Zhou (2010) incorporated the normalized difference vegetation index (NDVI) for Europe and China, respectively, to address the issue of land cover in their respective regions. NDVI measures vegetation coverage by comparing Red and Near-

Infrared bands of reflectance in satellite imagery, utilizing the fact that healthy vegetation reflects NIR and absorbs Red wavelengths of light. Higher NDVI values correspond to more vegetation-rich coverage (Benavidez 2018).

Significance and Objectives

Soil erosion is an increasingly serious issue in the United States. The issue of soil loss due to erosion is typically assessed on an annual scale. However, due to improvements in methods with increasing soil erosion research, intra-annual fluctuation can now be assessed. Using in-situ measurements for overall stream discharge and sediment concentrations along with RUSLE gross soil loss calculations, this thesis calculates monthly SDR values for the Senachwine Creek at Chillicothe, IL watershed for an average hydro-climatological crop-harvest season of May to October (NASS 1997, NASS 2010), the temporal and spatial scales of which RUSLE factors are best applied (Wischmeier and Smith 1978; Renard et al. 1997). In doing so, the thesis maintains the objective of correlating SDR fluctuation to changes in seasonal land and vegetation coverage in addition to fluctuations in precipitation across the watershed. In addition, it attempts to answer whether seasonal land and vegetation coverage play a major contributing role in the percentage of eroded sediment being permanently removed from the watershed through stream discharge.

DATA AND METHODS

Study Area

To assess the sediment delivery ratio (SDR), the study area of choice is the watershed draining to USGS stream gauge 055597000, Senachwine Creek at Chillicothe, Peoria County, IL. This site was chosen mainly as a result of data availability. The stream gage at Senachwine Creek records suspended sediment concentration and discharge, which are required for calculating the sediment yield. Furthermore, the area draining to this gage is dominated by agricultural lands, the original land cover type for which USLE and RUSLE were originally created to estimate total soil erosion losses (Wischmeier and Smith, 1978; Renard et al. 1997; Renard et al. 1994). The watershed covers an area of 84.50 square miles (USGS 2019a), which also fits within the spatial scale for which RUSLE soil loss estimates are most accurate (Renard et al. 1997).

The watershed traverses Peoria County, Marshall County, and a sliver of Stark County (White et al. 2008). The dominant soil type is mollisol, characterized as agricultural soil made highly productive due to a very fertile, organic rich surface layer. The next dominant soil type in the area is Drummer soil, an Alfisol, which consists of very deep, poorly drained soils that formed in 1-1.5 meters of loess or other silty material in the underlying stratified, loamy, glacial drift. Alfisol in general is characterized as highly fertile and productive agricultural soils in which clays often accumulate below the surface. Alfisol is typically found in humid and sub-humid climates (Wall and Allmon 2014). Moraines, formed during the Wisconsin Episode glacier, border the Senachwine Creek watershed as well as exist within the watershed at lower elevations. The Providence Moraine borders to the West and the Eureka Moraine borders to the East.

The entire upland surface of the watershed is covered by 8-12 feet of loess where it is not eroded away. Loess in general comprises the main source of sediment in overland flow.

Silt is transported easily in the watershed, moving sediment out of the watershed and depositing in the Peoria lake region below the watershed (White et al. 2008).

The climate of Chillicothe is typical of Central Illinois. The average normal monthly temperatures range from 32 ˚F in January to 87 ˚F in July. The normal monthly total precipitation ranges from 2.0 inches in February to 4.6 inches during May (Average Weather in Chillicothe Illinois, United States 2019). Figure 1 details a monthly breakdown of both average monthly temperature and total precipitation.

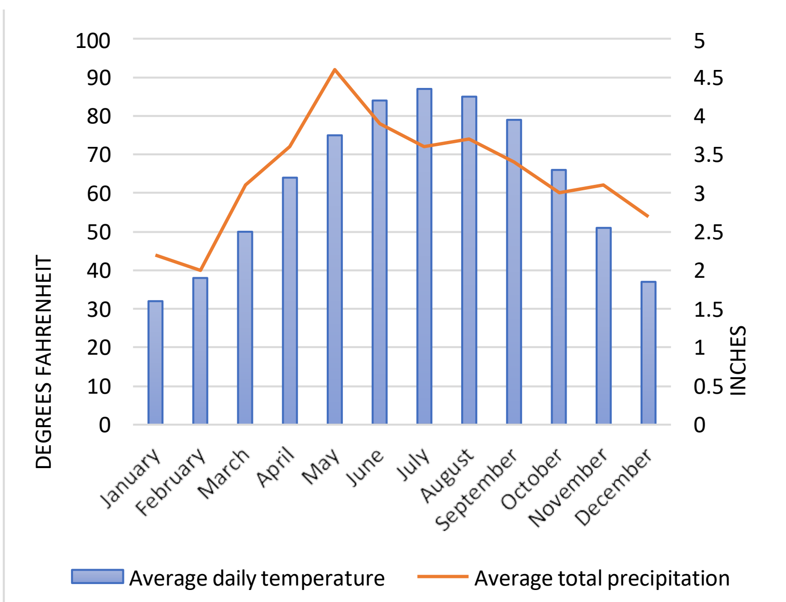

Figure 1. Average monthly temperature and total precipitation of Chillicothe, IL.

The economy around the agricultural lands of Illinois is dominated by corn. Most of the crop is sold as grain and livestock feed, but it is also processed to produce corn syrup, starch, and fuel alcohol. Corn is typically planted beginning mid-April, continuing through June and is typically harvested beginning in October until the end of November

(Kowalski 2019a). Soybeans are the second most farmed product, followed distantly by hay, wheat, rye, oats, and grain sorghum (Illinois State Agricultural Overview 2006).

Soybeans are typically planted soon after corn in late April though the end of June and are harvested typically in late September through the end of November (Kowalski 2019b). Apples are the most important fruit crop, followed by melons and peaches.

Other vegetable crops in addition to sweet corn are asparagus, cabbage, lima beans, and snap beans (Illinois State Agricultural Overview 2006).

Consequently, the watershed has a predominant land cover of cultivated crops, covering 72.7% of the total area. The latter land cover is followed by deciduous forest at 18.0%, developed open space at 3.92%, and pasture/hay coverage at 3.12%. Figure 2 and Table 2 describe these breakdowns in more detail. The watershed has a relief of 135 meters, with elevation ranging from 139-274 MASL (see Figure 3).

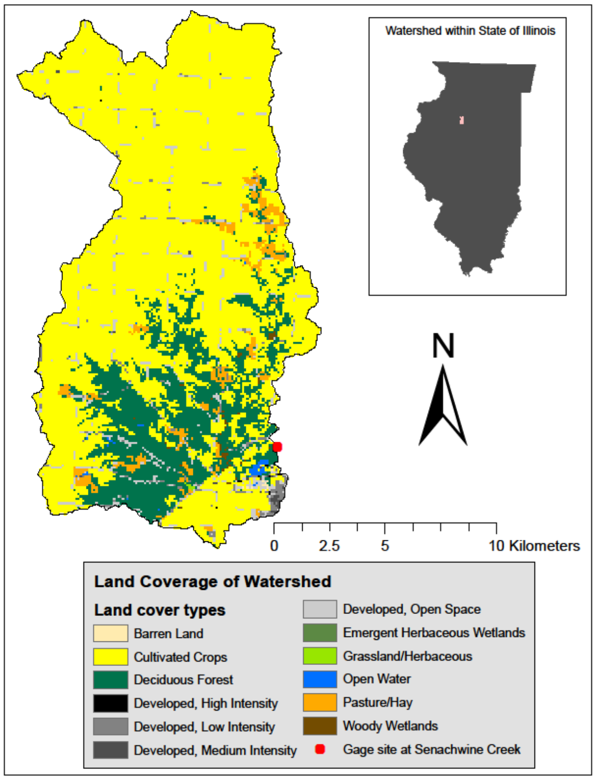

Figure 2. Land Cover Map of Watershed with Inset of Location within Illinois

Land cover type	Land cover percentage
Open Water	0.27
Developed, Open Space	3.92
Developed, Low Intensity	1.26
Developed, Medium Intensity	0.20
Developed, High Intensity	0.06
Barren Land	0.06
Deciduous Forest	18.05
Grassland/Herbaceous	0.04
Pasture/Hay	3.12
Cultivated Crops	72.74
Woody Wetlands	0.29
Emergent Herbaceous Wetlands	0.00

Table 2. Land coverage type and percentages of watershed

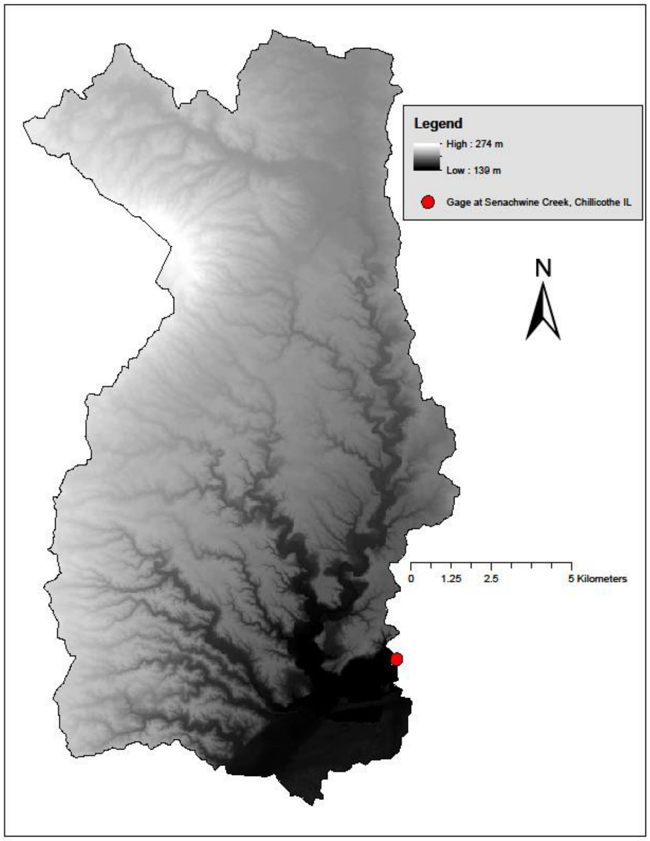

Figure 3. Topography of the studied watershed area

The normal mean monthly discharge from Senachwine Creek peaks in May at 213 ft^3/s to 8.1 ft^3/s and 9.7 ft^3/s during August and September, respectively (Figure 4). For this research, the year 2011 was chosen for analysis as it most closely resembled the average monthly hydrologic conditions of the watershed (Figure 4).

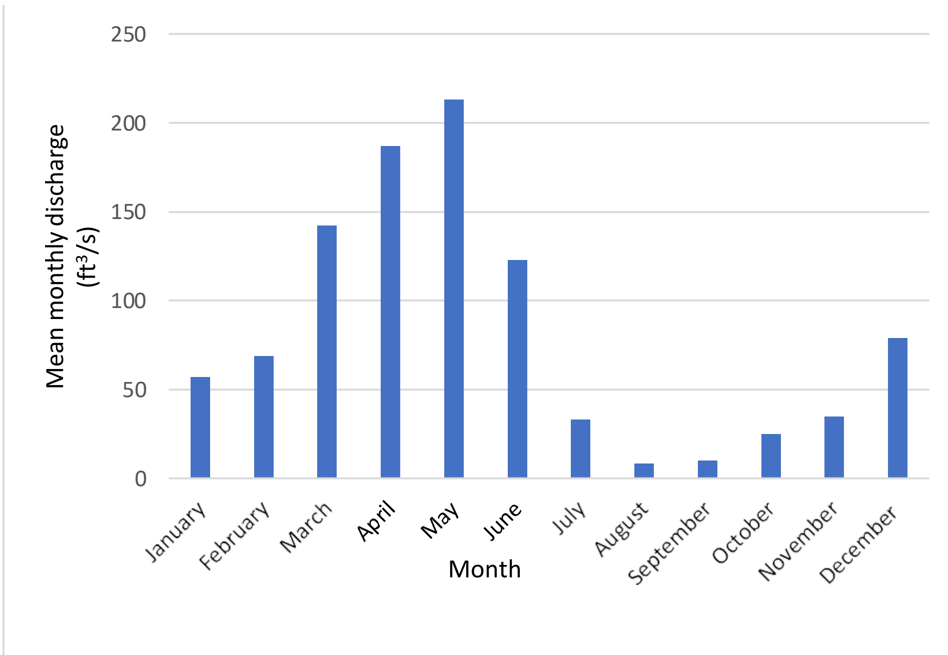

Figure 4. Normal mean monthly discharge for Senachwine Creek stream gage.

Sediment yield

The sediment yield component of the SDR will be calculated using the suspended sediment concentration (SSC) data collected by the USGS stream gage 055597000, Senachwine Creek at Chillicothe (USGS 2019a). This data will be obtained for each month between May and October 2011, in metric tons for the study area. This data will be used as the numerator component of the SDR.

RUSLE Overview

The soil erosion loss component for the SDR, the denominator, will be calculated using soil loss equations. The RUSLE formula for calculating soil erosion is best utilized when applied to relatively homogenous areas, which is typically said to be less than 1 square kilometer (Wischmeier and Smith 1978; Renard et al. 1997; Evans and Seamon 1997), which is appropriate for the study area selected. The original USLE equation from Wischmeier and Smith (1978) is given as follows:

$$A = R * K * L * S * C * P, \qquad (1)$$

where A is soil loss (mass/area/unit time), R is Rainfall erosivity factor, K is Soil erodibility factor, L is the hillslope length factor, S is the hillslope gradient factor, C is the cropping management factor, and P is the erosion control practice factor. These factors are calculated and compared to those based on a conceived unit plot of 22.1 m long, 1.83m wide, with a slope of 9% (Benavidez 2018; Renard et al. 1997; Wischmeier and Smith 1978). In this study, as in others, the P factor was assumed to have a default value of 1 as neither secondary data on erosion management support practices were available, nor was field data collection possible. Typical support practices include various tillage, cropping and drainage practices designed to minimize soil erosion from rainfall and irrigation-induced runoff (USDA 2013). . Each remaining factor and its units are described as follows.

R factor

The R factor of the RUSLE formula represents the erosive action of rainfall on the soil. Additional soil erosion from mis-managed irrigation is also possible although this requires local field data on specific irrigation measures and applications throughout the growing season (USDA 2013). As this data was not available it was not considered in this research. Monthly R-factor values will be obtained from the R-factor calculator provided by the EPA using the watershed centroid as the target location (EPA 2019). The R factor is dependent on long-term rainfall per location. The R factor is a function of the mean monthly multiple of storm kinetic energy and maximum 30-minute intensity and can be calculated on a monthly timescale (Renard et al. 1997; Wischmeier and Smith 1978). RULSE adds a correction component to the original USLE R factor in order to reflect the effect of raindrop impact for flat slopes striking water on a pooled surface (Renard et al. 1997). The units typically given for the R factor as stated by Renard et al. (1997) are hundreds of foot ton-force (tonf) inch per acre per hour per year. Multiplying by 17.02 will give SI units of megajoule millimeter per hectare per hour per year. The equation for R (Wischmeier and Smith 1978; Renard et al. 1997) is given below, altered to reflect the monthly timescale used in this study:

$$R = [\ \sum(EI_{30})i\ ] / N \text{ for number of storms in an N-month period} \qquad (2)$$

$$EI_{30} = E \times I_{30} \qquad (3)$$

$$E=916+331\times\log_{10}I \qquad (4)$$

where I is the intensity (in h^{-1}), EI_{30i} is EI_{30} for storm i, and j is the number of storms in an N-month period (Benavidez et al. 2018; Renard et al. 1997). The units of R in US customary units are given as hundreds of ft*tonf*in/ac/hr, multiplying by 17.02 to get SI units of MJ*mm/ha/hr/yr (Foster et al. 1981).

K factor

The soil erodibility factor (K) represents the influence of different soil properties on the corresponding slope’s susceptibility to erosion (Renard et al. 1997). Data incorporating the soil erodibility factor will be obtained from ESRI in the form of a 30m resolution raster generated from the NRCS soil survey program (NRCS 2019). The K factor can be defined as the "mean annual soil loss per unit of rainfall erosivity for a standard condition of bare soil, recently tilled up-and-down slope with no conservation practice," (Morgan 2005). This factor used in RUSLE is adjusted to account for seasonal changes such as freezing conditions, soil consolidation, and soil moisture. Higher K-factor values indicate the soil's higher susceptibility to soil erosion (Benavidez 2018). The equation adopted by Renard et al. (1997) incorporates textural information, organic matter, information regarding soil structure, and profile permeability all within the K-factor. The actual equation set forth by Wischmeier and Smith (1978) and utilized by Renard et al. (1997) is described below,

$$M = \text{silt} \times (100 - \text{clay}) \tag{5}$$

$$K = \{[2.1 \times M^{1.14} \times (10^{-4}) \times (12 - a)] + [3.25 \times (b - 2)] + [2.5 \times (c - 3)]\} \div 100 \tag{6}$$

where M is the particle-size parameter; silt is silt percent as well as percent of very fine sand (0.1 to 0.05mm); clay is the clay percent; a is the organic matter as a percent; b is the soil structure code used in soil classification – 1 for very fine granular, 2 for fine granular, 3 for medium or coarse granular, and 4 for blocky, platy or massive; and c is the profile permeability class, where 1 is for rapid, 2 for moderate to rapid, 3 for moderate, 4 for slow to moderate, 5 for slow, and 6 for very slow. The units for the K-factor per unit of rainfall erosivity in US customary units is T*ac*hr/hundreds of ac/ft/tonf/in, multiplying by 0.1317 to receive SI units of T*ha*hr/ha/MJ/mm (Foster et al. 1981).

L and S factors

The L and S factors represent the effect of the slope's length and steepness on sheet, rill, and inter-rill erosion by water. The slope length (L) and slope steepness (S) factors will be calculated from a 30m resolution digital elevation model (DEM) for the watershed available from the USGS National Geospatial Program (USGS 2019b). The factors are typically taken together and is given as a ratio of expected soil loss from a field slope relative to the unit plot used in USLE (Benavidez 2018). While the USLE method of calculating slope length and steepness were originally applied at the unit plot and field scale, RUSLE extends this to a one-dimensional hill slope scale, with different equations depending on whether the slope has a gradient of more than 9% (Renard et al. 1997; Wischmeier and Smith 1978). For the sake of simplicity in this study, the L and S factors are calculated as follows:

$$L = 1.4\ (A_s/22.13)^{0.4} \qquad (7)$$

$$S = (\sin \beta\ /\ 0.0896)^{1.3} \qquad (8)$$

where A_s is the specific contributing area (m^2/m) and β is the slope angle in degrees.

C factor

The C factor in RUSLE is also known as the cover and management factor (Benavidez et al. 2018). The cover and management factor can be found by generating an NDVI raster of the watershed in ArcMap that is representative of each month of the study year from 30m Landsat 8 imagery from the USGS EarthExplorer program (USGS 2019c). It is defined as the ratio of soil loss from a field with a particular cover and management to that of a field under "clean-tilled continuous fallow" (Wischmeier and Smith 1978). RUSLE enhances this component by adding sub-factors into consideration

– prior land use, canopy cover, surface cover, surface roughness, and soil moisture. This factor is the most updated, dividing each year in rotation into 15-day intervals, while calculating soil loss ratios for each period, and recalculating every time a change in tillage operation occurs. This allows for improved estimates of soil loss changes as they occur intra-annually. The above description is described in detail in Renard et al. (1994). In further adaptations of RUSLE, the C factor increasingly incorporates the Normalized Difference Vegetation Index (NDVI) to account for canopy and ground vegetation coverage (Benavidez et al. 2018; Van der Knijff, Jones, and Montanarella 2000). The equation for the C factor as used by Van der Knijff, Jones, and Montanarella (2000) is as follows,

$$C = \exp \{2 [NDVI / (1 - NDVI)]\} \qquad (9)$$

where NDVI is a normalized ratio varying between -1 and 1 that compares the amount of light reflected from the surface in the Red and Near-Infrared spectrums, utilizing the fact that vegetation reflects mainly NIR bands and absorbs the Red. The equation for NDVI is as follows,

$$NDVI = [NIR - Red] / [NIR + Red] \qquad (10)$$

where NIR is the measured reflectance in the near-infrared part of the spectrum, and Red is the measured reflectance in the Red part of the light spectrum. Using NDVI, researchers have the advantage of incorporating sub-annual C factors, which allows for assessment of coverage of seasonal erosion and identifying important periods of soil erosion risk throughout the year (Ferreira and Panagopoulos 2014).

Sediment Delivery Ratio

For calculation of the SDR, this proposal follows the methodology laid out by Evans and Seamon (1997), changing the units to reflect the monthly timescale. The SDR is defined as

$$D = (Y/T) * 100 \qquad (11)$$

where D is the sediment delivery ratio as a percent; Y is the sediment yield (metric ton/month), and T is the total soil erosion loss (metric tons/month). The sediment yield will be taken from the aforementioned in-situ data recorded by the stream gage at the watershed outlet while the total soil erosion loss will be estimated using the RUSLE method described.

RESULTS

R factor

Using the EPA Rainfall Erosivity (R-factor) calculator, the R-factor was calculated monthly between May and October of 2011 for the watershed. In doing so, the geographic location of Latitude -89.55 and Longitude 41.00 was used, as it roughly corresponds to the center of the watershed. The R-factor values taken from the EPA site range from 10.36 ft/tonf/in/ac/hr/yr to 35.79 ft/tonf/in/ac/hr/yr, which correspond to October and July, respectively. The R-factor starts at 19.76 ft/tonf/in/ac/hr/yr for the month of May, steadily increasing until July, then reaches its lowest value in October (see Figure 5). These values were converted to metric units of MJ*mm/ha/hr/yr for the final RUSLE output.

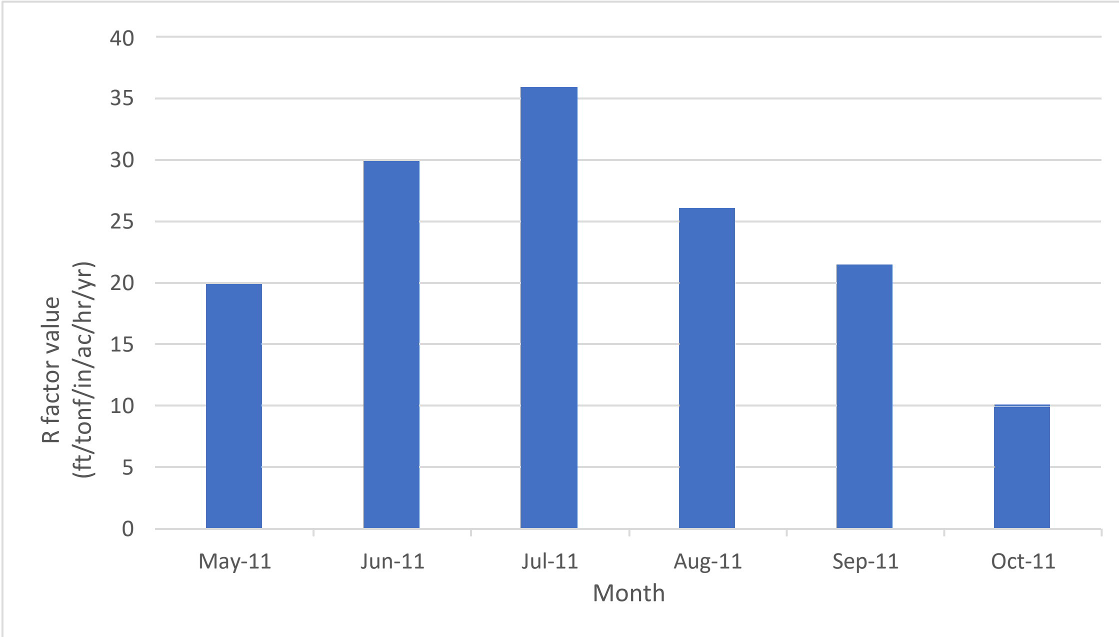

Figure 5. Bar chart of Rainfall Erosivity (R) factors from May – October 2011

K factor

The range of K-factor values (unit-less) is 0.020 to 0.540 across the watershed. The lowest values are mainly across the south-central area of the watershed. Higher values are also found through parts of the northern portion of the watershed, with the highest values spanning from central to northcentral areas along the main stream channel.

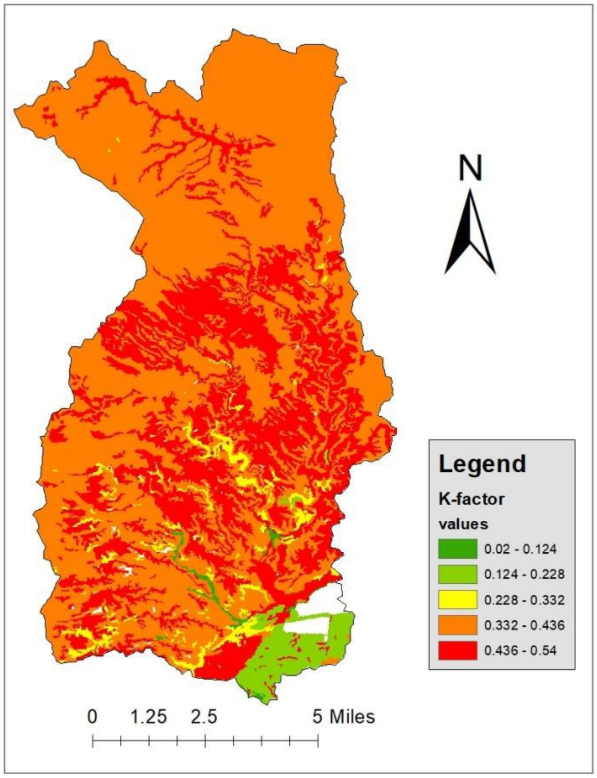

Figure 6. Soil Erodibility (K) factor for watershed

L and S factors

In calculating the L and S factors together, a DEM of the watershed was utilized to create a Slope raster, Flow Accumulation raster, and through Map Algebra, a final LS-factor raster (see Figure 7). Revealing the susceptibility of erosion due to slope length and steepness, the watershed maintains a range of values from 0 to 23.168 (units of degrees*m^2/m), with an overwhelming majority of values falling at or below 0.169. The areas with the highest values correspond to areas where rivers and streams have carved out the landscape to a more drastic degree, while lower values correspond to the overwhelming expansive flat areas of agricultural productivity throughout the watershed (see Figure 7).

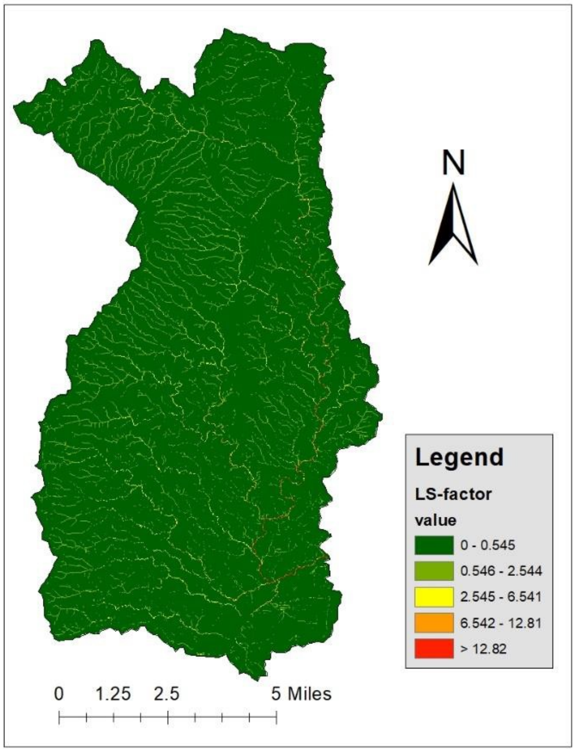

Figure 7. Length-Slope (LS) factor for watershed

C factor

The monthly C-factors (see Figure 9) were calculated through a Map Algebra expression applied on monthly NDVI scenes (see Figure 8). These monthly NDVI scenes were in turn created by averaging the NDVI scene dates within each month, or for the case of June, the last scene of May and the first scene of July (due to lack of data availability), through Map Algebra. A breakdown of which Landsat scenes were used for monthly NDVI calculations is detailed below (Table 3).

NDVI scene month	NDVI raster(s) used for monthly average	Path	Row
May	5/1/2011	24	31
	5/17/2011	24	31
June	5/17/2011	24	31
	7/4/2011	24	31
July	7/4/2011	24	31
	7/20/2011	24	31
August	8/21/2011	24	31
September	9/15/2011	23	32
October	10/1/2011	23	32
	10/24/2011	24	31

Table 3. List of dates and scenes used for average monthly C-factor calculations

The monthly NDVI scenes varied both temporally and spatially across the watershed within the months of analysis. They share an inverse relationship with the C-factor – trends in NDVI are directly opposite to the trends in C-factor values. Therefore, focus will stay on NDVI trends, which can then be extrapolated to be opposite of C-factor trends.

A typical temporal trend consists of lower NDVI values in May, increasing up until August, with a retreat in values through October. As NDVI detects vegetation coverage, this also corresponds with the crop-harvest season of Illinois. There is relatively bare land across the watershed as the crop-harvest season is just beginning in May; this is especially true outside the south-central to east-central portions of the watershed where the main stream channels are located. Afterwards, there is peak vegetation coverage in August, and harvesting occurring from end of September through

October to return back to a bare land coverage extent similar to that of May (Illinois State Agricultural Overview 2006, NASS 1997, NASS 2010). NDVI values duly peaked in August with a high value of 0.952, and dropped to a low of -0.396 in October post-harvest. Spatially, across all 6 months, there is a trend of higher values as one moves closer to the Southcentral portion of the watershed. The Southeast portion is excluded from these high trends, consisting of lower values throughout the 6-month time period. In terms of NDVI averages across the watershed, May and October maintained the lowest NDVI averages at 0.318 and 0.385, respectively. Conversely, July and August maintained the highest NDVI averages at 0.761 and 0.818, respectively. A visual breakdown of NDVI values and C-factor values are detailed in proceeding figures (see Figures 8 and 9, respectively).

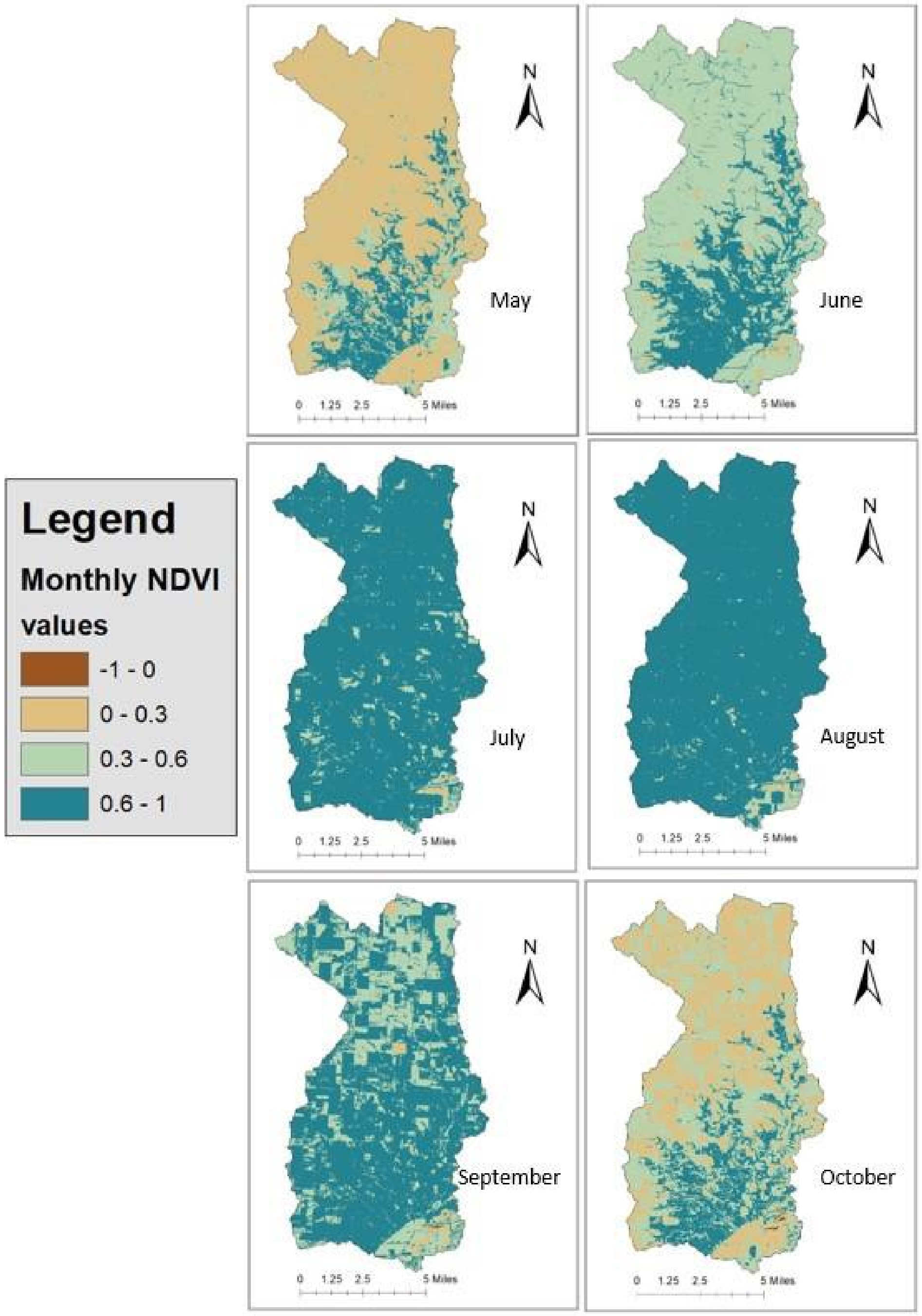

Figure 8. NDVI composites for May – October 2011

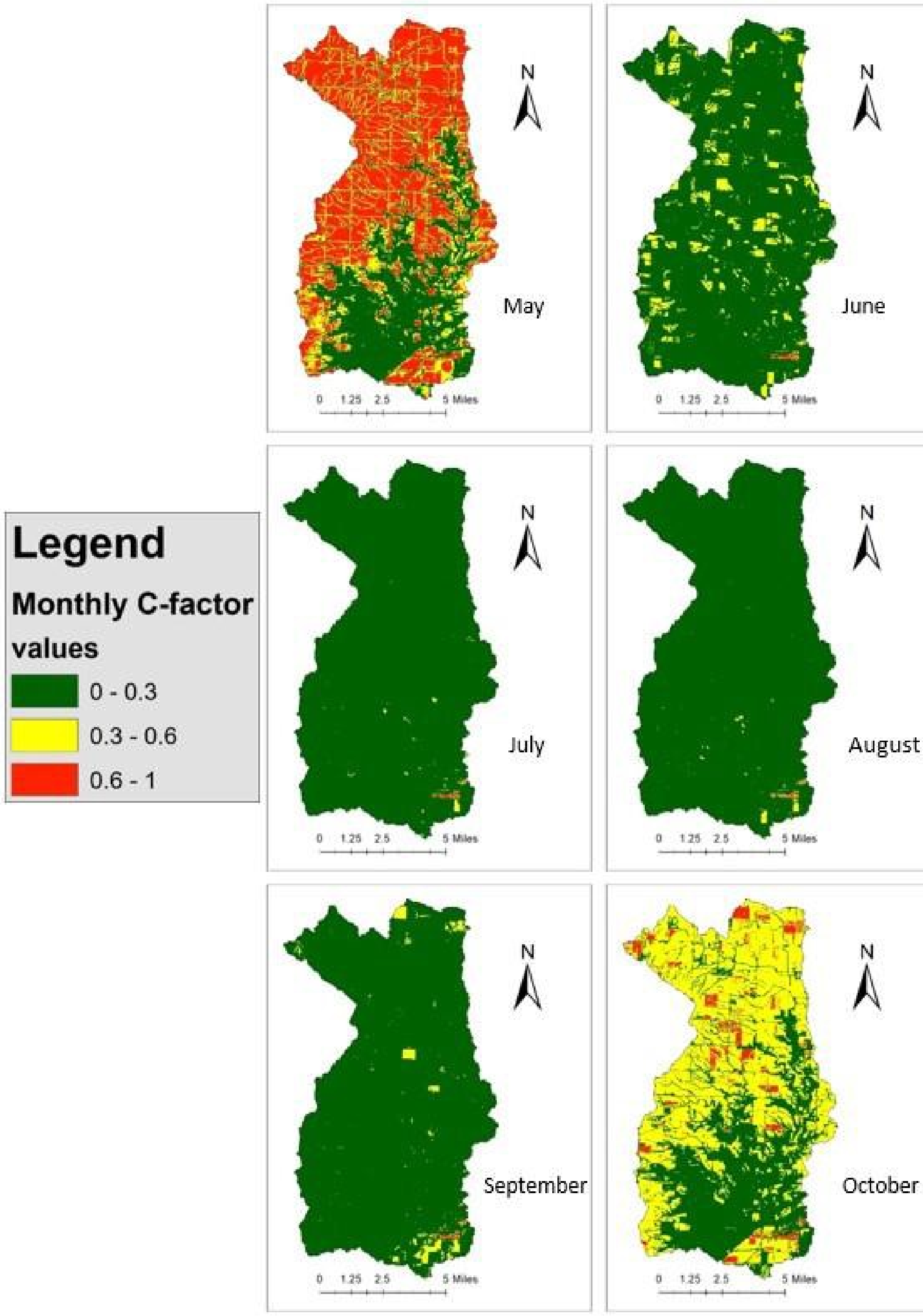

Figure 9. C factor values for May – October 2011

RUSLE estimated gross soil erosion

Multiplying together the rasters for the rainfall erosivity, soil erodibility, length and slope, and cover/management factors together gives monthly erosion totals in Tons/ha for the entire watershed draining out of Senachwine Creek outlet point. Based on the monthly outputs, there exists a general trend temporally of decreased erosion between the onset of the crop-harvest season and August – the peak of crop production. Afterwards, there is a general increase in erosion totals until the end of the crop-harvest season, when harvesting reaches its peak. Spatially, there is an observed pattern of increased erosion away from the southcentral portion of the watershed. This is especially noticeable for the months of May, June, September and October, outside the months of highest agricultural productivity. To break down the distribution of estimated average and total soil erosion by month, May maintains the highest average and total erosion values with 1.041 T/ha and 22,780 T, respectively. The average and total erosion values decrease until August, dropping to an average of 0.0189 T/ha and a total of 414 T. Afterward, these values increase through October, which maintains an average of 0.3768 T/ha and a total erosion of 8250 T. Figure 10 shows the spatial distribution of soil loss across the entire watershed on a monthly basis.

Suspended Sediment Yield

Unlike the estimated monthly gross soil erosion, the suspended sediment yield (SSY) trend shows a linear decrease across the crop-harvest season, starting at 7826.6 metric tons in May 2011 and dropping down to 0.0025 metric tons by October 2011 (see Figure 11). To break this down further, June and July maintain SSYs of 1988.2 metric tons and 210.7 metric tons respectively. Additionally, August and September maintain SSYs of 11.9 metric tons and 0.69 metric tons, respectively.

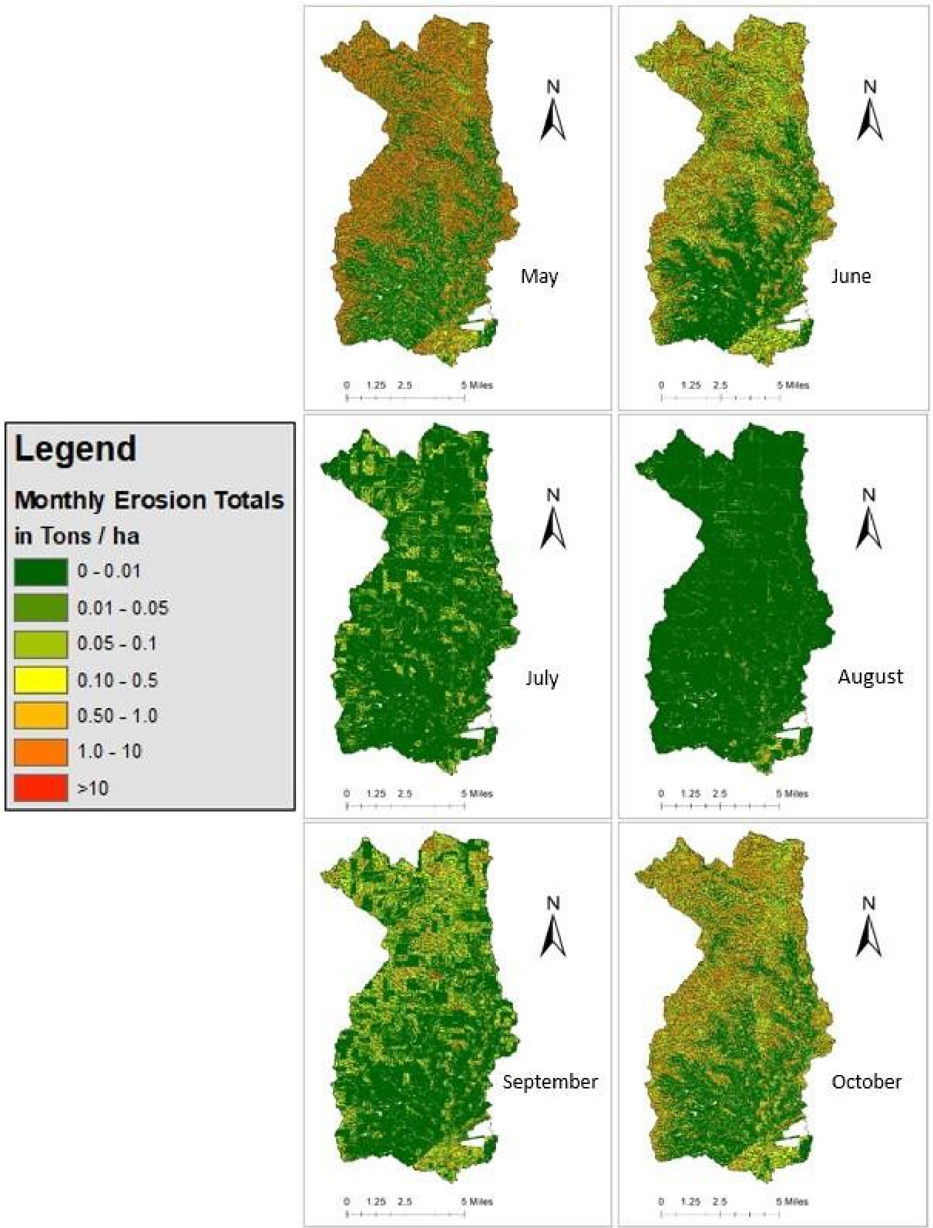

Figure 10. The watershed monthly erosion totals in T/ha for May – October 2011

DISCUSSION

RUSLE Estimated Gross Soil Erosion

Given the described pattern of estimated gross soil erosion, the main takeaway is the alignment of soil erosion with barren land coverage across the watershed. Assuming NDVI values less than 0.3 typically reflect barren land cover, then 63% of the land is bare in May, decreasing rapidly to 0.47% and 0.57% in July and August, respectively. Then, the bare land coverage rapidly increases back to 41.5% by October (see Figure 11). This mirrors the onset of the cropping season – before planting occurs, the peak of crop production in August, and of the post-harvesting season. As the extent of vegetation coverage detected by NDVI resembles a fluctuating pattern, so does the gross soil erosion estimates given by the RUSLE equation. It is important to note that the exclusion of the erosion control factor (P), assumed as a default value of 1, would likely result in generating soil erosion estimates above those actually occurring across the watershed. Various tillage, cropping and drainage practices may be in place across the study area to limit soil erosion to some degree. Furthermore additional irrigation may increase the soil erosion above the estimates given here as an addition to the rainfall erosivity (USDA 2013). However, there were no readily available data sets covering these factors and in-situ measurements remained outside the scope of this research.

Suspended Sediment Yield

The decreasing linear trend in the SSY aligns well with normal precipitation measurements across the region (see Figure 1), which peak around May, and steadily decrease until the end of the crop-harvest season in October. At the beginning of the crop-harvest season, large SSY values can most likely be attributed to not only higher precipitation levels but also to the barren land percentage as shown through NDVI. This indicates both precipitation and vegetation cover contributing towards higher SSY values for the beginning and middle of the crop-harvest season. As vegetative cover starts to increase across the watershed due to cropping practices, a noticeable decrease in SSY is apparent. This may explain why SSY continues to decrease while precipitation typically increases between July and August. However, the increase in barren land cover towards the end of the season does not seem to affect the SSY to the same degree as precipitation, as SSY values continue to decrease dramatically as barren land percentages decrease along with it. Therefore, while the hypothesis of increased vegetation land cover and precipitation affects SSY values can be confirmed, the data seems to more strongly support precipitation as the primary controlling factor on SSY.

Sediment Delivery Ratio

The SDR, composed of SSY as the numerator and RUSLE's estimated gross soil erosion as the denominator, reveals a fluctuating pattern across the crop-harvest season. May maintains an SDR of 34%, dropping to 27% in June. This is followed by a slight increase to 30% in July with a steep drop to 2.9% in August and decreasing values below 1% in September and October. The ratio components of estimated gross soil erosion and SSY, along with barren land percentage (NDVI < 0.3) is shown in Figure 11. The fluctuating pattern is hard to attribute directly to vegetation coverage and/or precipitation at first glance but breaking down the individual components of the SDR reveals trends that support the general hypothesis of vegetation cover and precipitation affecting the ratio as a whole. Mainly, that vegetation/barren land cover controls the overall estimated soil erosion (RUSLE) from the watershed, while precipitation primarily affects the suspended sediment yield, with minor effects from barren land cover extent in the beginning and middle of the crop-harvest season. This signifies that the hypothesis of vegetation cover affecting the SDR should not be rejected.

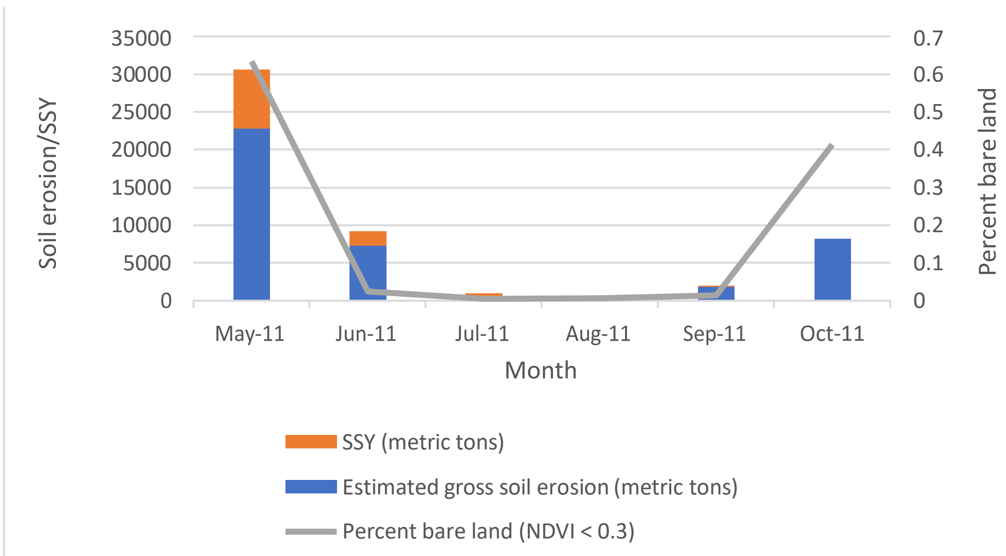

Figure 11. Estimated gross soil erosion and suspended sediment yield compared to the percent of bare land cover

Potential impacts of climate change

As the rainfall erosivity factor plays a major role in controlling seasonal soil erosion, changes in precipitation over time may potentially affect future soil erosion across the watershed. For example research has shown that the Midwest US region has experienced a 10% - 15% increase in precipitation between 2001 and 2012In addition, heavy rainfall events within this same time period (defined as the heaviest 1% of all storms recorded), have also increased by 30%(Melillo, Richmond, and Yohe 2014). Both of these recent trends suggest that potential soil erosion, sediment yield and the overall SDR of the watershed will continue to increase should these trends continue over the next few decades. Therefore, understanding how soil erosion occurs and finding ways to manage this is of ever-growing importance.

CONCLUSION

By analyzing monthly sediment delivery ratios (SDRs) for an agriculture dominated watershed, this thesis aimed to address whether precipitation and vegetation land cover changes affect SDR fluctuations throughout an average hydroclimatological crop-harvest season. Furthermore, this thesis addressed how the individual components of the ratio, suspended sediment and gross soil erosion estimates, are each potentially affected by these two variables. This research finds that the SDR is directly affected both by precipitation and land cover, confirming the general hypothesis. In addition, the extent to which these factors affect each component of the SDR was able to be assessed. First, the suspended sediment yield is primarily controlled by precipitation decrease throughout the crop-harvest season, with moderate alignment with decreasing barren land coverage up until the peak of the crop season in August. Secondly, the estimated gross soil erosion resembles a pattern that most closely matches the extent of barren land cover decrease, then increase, throughout the crop-harvest season. In this manner, the SDR reveals a slight fluctuating pattern that is attributed to the trends of each component composing the SDR – estimated gross soil erosion and suspended sediment yield, confirming the original hypothesis.

Further study into the concept of monthly SDRs and their relationship with land cover and precipitation can take a few different avenues of exploration. Firstly, further investigation can consist of statistical analysis of both precipitation and land cover correlation with the sediment delivery ratio at large, as well as estimated gross soil erosion and suspended sediment yield. Additional data concerning irrigation usage and support practice factors could also be collected to update the RUSLE equation and assess possible impacts on estimated soil erosion losses from the cropped land cover areas. In addition, assessing different watersheds, both nationally and internationally, can be undertaken to add to the reproducibility of these results. Lastly, the study of economic impacts of fluctuating sediment delivery ratios can help advise how to more efficiently manage erosion practices throughout a typical crop-harvest season.

In light of creating a sustainable future of food production, and regarding an increasingly changing climate, much focus has centered on the effects of soil erosion in agricultural landscapes. The amount of sediment eroded that is permanently discharged from a watershed intrinsically ties into this issue of erosion and its consequences toward sustainable food production. Therefore, this thesis hopes to shed light on the impactful relationships between both precipitation and land cover and their effects on the overall sediment eroded and the amount of it permanently leaving the agricultural watershed.

REFERENCES

Adornado, H. A., M. Yoshida, and H. A. Apolinares. 2009. Erosion Vulnerability Assessment in REINA, Quezon Province, Philippines with Raster-based Tool Built within GIS Environment. *Agricultural Information Research* 18 (1):24–31.

Aksoy, H., and M. L. Kavvas. 2005. A review of hillslope and watershed scale erosion and sediment transport models. *Catena* 64 (2-3):247–271.

Arnoldus, H. M. 1980. *An approximation of the rainfall factor in the Universal Soil Loss Equation*. Chichester, UK: Wiley.

Arsenault, C. 2014. Only 60 Years of Farming Left If Soil Degradation Continues. *Scientific American*. https://www.scientificamerican.com/article/only-60-years-of-farming-left-if-soil-degradation-continues/ (last accessed 14 November 2019).

Benavidez, R., B. Jackson, D. Maxwell, and K. Norton. 2018. A review of the (Revised) Universal Soil Loss Equation ((R)USLE): with a view to increasing its global applicability and improving soil loss estimates. *Hydrology and Earth System Sciences* 22 (11):6059–6086.

Blanco, H., and R. Lal. 2010. *Principles of soil conservation and management*. Dordrecht: Springer.

Boyce, R. C. 1975. Sediment routing with sediment delivery ratios. Present and Prospective Technology for Predicting Sediment Yields and Sources. U.S. Department of Agriculture, Publication ARS-S40 pp. 61-65.

Cedar Lake Ventures. 2019. Average Weather in Chillicothe, Illinois, United States, Year Round. *WeatherSpark*. https://weatherspark.com/y/12684/Average-Weather-in-Chillicothe-Illinois-United-States-Year-Round (last accessed 19 March 2020).

Colman, E. A. 1954. *Vegetation and watershed management; an appraisal of vegetation management in relation to water supply, flood control, and soil erosion*. New York: Ronald Press Co.

da Silva, A. M. 2004. Rainfall erosivity map for Brazil. *Catena* 57 (3):251–259.

David, W. P. 1988. Soil and Water Conservation Planning: Policy Issues and Recommendations. *Philippine Journal of Development*. https://ideas.repec.org/p/phd/pjdevt/jpd_1988_vol__xv_no 1-c.html (last accessed 8 November 2019).

deCarvalho, D. F., V. L. Durigon, M. A. H. Antunes, W. S. D. Almeida, and P. T. S. D. Oliveira. 2014. Predicting soil erosion using Rusle and NDVI time series from TM Landsat 5. *Pesquisa Agropecuária Brasileira* 49 (3):215–224.

Demissie, M., R. Xia, L. Keefer, and N. Bhowmik. 2004. The Sediment Budget of the Illinois River. *Illinois State Water Survey*, *Contract Report 2004- 13*. Champaign, IL.

Desmet, P. J. J. and Govers, G. 1996. A GIS procedure for automatically calculating the USLE LS factor on topographically complex landscape units. *Journal of Soil and Water Conservation* 51: 427–433.

Dymond, J. R. 2010. Soil erosion in New Zealand is a net sink of CO2. *Earth Surface Processes and Landforms* 35 (15):1763–1772.

EarthExplorer. *United States Geological Survey*. https://earthexplorer.usgs.gov/ (last accessed 29 October 2019).

Easterling, D. R., and T. R. Karl. 2001. Climate change impacts on the United States: the potential consequences of climate variability and change. *Choice Reviews Online* 38 (11).

Ebrahimzadeh, S., M. Motagh, V. Mahboub, and F. M. Harijani. 2018. An improved RUSLE/SDR model for the evaluation of soil erosion. *Environmental Earth Sciences* 77 (12).

El-Swaify, S. A. and Dangler, E. W. 1976. Erodibilities of selected tropical soils in relation to structural and hydrologic parameters. *Soil Conservation Society of America*: 105-114.

El-Swaify, S. A., Gramier, C. L., and Lo, A. 1987. Recent advances in soil conservation in steepland in humid tropics. *Proceedings of the International Conference on Steepland Agriculture in the Humid Tropics*. Kuala Lumpur: MADI.

EPA. 2016. Climate Change Indicators: Weather and Climate. *EPA*. https://www.epa.gov/climate-indicators/weather-climate (last accessed 5 November 2019).

EPA. 2019. Low Erosivity Waiver (LEW). Available at https://lew.epa.gov/ (last accessed 5 November 2019).

Evans, J. E., and D. E. Seamon. 1997. A GIS Model to Calculate Sediment Yields from a Small Rural Watershed, Old Woman Creek, Erie and Huron Counties, Ohio. *Ohio Journal of Science* 97 (3):44–52.

FAO. SLM practices. Food and Agriculture Organization of the United Nations. http://www.fao.org/land-water/land/sustainable-land-management/slm-practices/en/ (last accessed 4 November 2019).

Fagnano, M., N. Diodato, I. Alberico, and N. Fiorentino. 2012. An overview of soil erosion modelling compatible with RUSLE approach. Rendiconti Lincei 23 (1):69–80.

Ferreira, V., and T. Panagopoulos. 2014. Seasonality of Soil Erosion Under Mediterranean Conditions at the Alqueva Dam Watershed. *Environmental Management* 54 (1):67–83.

Foster, G. R., D. K. McCool, K. G. Renard, and W. C. Moldenhauer. 1981. Conversion of the universal soil loss equation to SI metric units. *Journal of Soil and Water Conservation* 36(6):355–359.

Gabriels, D. M., and W. M. Cornelis. 2015. Human-induced land degradation. *Land Use, Land Cover, and Soil Sciences* 3.

Gray, D. H., and A. T. Leiser. 1982. Biotechnical Slope Protection and Erosion Control. New York: Van Nostrand Reinhold Company.

Griffin, E. R., and J. D. Smith. 2001. Analysis of vegetation controls on bank *erosion rates, Clark Fork of the Columbia River, Deer Lodge Valley, Montana*. Reston, VA: U.S. Dept. of the Interior, U.S. Geological Survey.

Gruver, J. B. 2013. Prediction, Prevention and Remediation of Soil Degradation by Water Erosion. *Nature Education Knowledge* 4(12):2.

Hooke, R. L. 2000. On the history of humans as geomorphic agents. *Geology* 28 (9):843.

Illinois State Agricultural Overview. 2006. Washington, D.C.: US Department of Agriculture.

Kinnell, P. 2010. Event soil loss, runoff and the Universal Soil Loss Equation family of models: A review. *Journal of Hydrology* 385 (1-4):384–397.

Kowalski, C. 2019a. Corn Crop Planting and Harvest Seasons. *The Balance*. https://www.thebalance.com/corn-planting-and-harvest-seasons-809309 (last accessed 18 November 2019).

Kowalski, C. 2019b. When Is Soybean Season? A Commodity Investor's Guide to Trading Soy. *The Balance*. https://www.thebalance.com/soybean-planting-and-harvest-seasons-809258 (last accessed 18 November 2019).

Lamba, J., A. Thompson, K. Karthikeyan, and F. A. Fitzpatrick. 2015. Sources of fine sediment stored in agricultural lowland streams, Midwest, USA. *Geomorphology* 236:44–53.

Lee, G.-S., and K.-H. Lee. 2010. Determining the Sediment Delivery Ratio Using the Sediment-Rating Curve and a Geographic Information System–Embedded Soil

Erosion Model on a Basin Scale. *Journal of Hydrologic Engineering* 15 (10):834–843.

Ma, H. L., Wang, Z. L., and Zhou, X. 2010. Estimation of soil loss based on RUSLE in Zengcheng, Guangdong Province, Yangtze River. 41, 90–93.

Maner, S.B. 1962. Factors influencing sediment delivery ratios in the Blackland Prairie land resource area. US Dept. of Agriculture, Soil Conservation Service, Fort Worth, Texas.

Melillo, J. M., T. C. Richmond, and G. W. Yohe eds. 2014. *Climate Change Impacts in the United States: The Third National Climate Assessment*. Washington, D.C.: U.S. Government Printing Office.

Mindat. 2019. Definition of productive land. *Hudson Institute of Mineralogy*. https://www.mindat.org/glossary/productive_land (last accessed 14 November 2019).

Morgan, R. P. C. 2005. Soil Erosion and Conservation. *National Soil Resources Institute*. Cranfield University, https://doi.org/10.1002/9781118351475.

Morgan, R. P. C., and R. J. Rickson. 2011. *Slope stabilization and erosion control: a bioengineering approach*. London: Taylor & Francis Group.

Naipal, V., C. Reick, J. Pongratz, and K. V. Oost. 2015. Improving the global applicability of the RUSLE model – adjustment of the topographical and rainfall erosivity factors. *Geoscientific Model Development* 8 (9):2893–2913.

Nakil, M., and M. Khire. 2016. Effect of slope steepness parameter computations on soil loss estimation: review of methods using GIS. *Geocarto International* 31 (10):1078–1093.

NASS. 1997. *Usual planting and harvesting dates for U.S. field crops* 1st ed. Washington, D.C.: USDA.

NASS. 2010. *Usual planting and harvesting dates for U.S. field crops* 2nd ed. Washington, D.C.: USDA.

NRCS. 1998. Erosion and Sediment Delivery. Field Guide. Washington DC: USDA. https://efotg.sc.egov.usda.gov/references/public/IA/Erosion_and_Sediment_Delivery.pdf (last accessed 28 October 2019).

NRCS. 2019. USA Soils Erodibility Factor. *Overview*. https://www.arcgis.com/home/item.html?id=ac1bc7c30bd4455e85f01fc51055e58 6 (last accessed 18 November 2019).

Panagos, P., Ballabio, C., Borrelli, P., Meusburger, K., Klik, A., Rousseva, S., and Alewell, C. 2015. Rainfall erosivity in Europe. *Science of the Total Environment* 511: 801–814.

Renard, K.G., G.R. Foster, G.A. Weesies, D.K. McCool, D.C. Yoder. 1997. Predicting soil erosion by water: a guide to conservation planning with the revised universal soil loss equation (RUSLE). US Department of Agriculture. *Agricultural Handbook No. 703*.

Renard, K.G., G.R. Foster, D.C. Yoder, D.K. McCool. 1994. RUSLE revisited: status, questions, answers, and the future. Soil and Water Conservation Society. *Journal of Soil and Water Conservation* 49(3):213-220.

Renfro, G.W. 1975. Use of erosion equations and sediment delivery ratios for predicting sediment yield. Present and Prospective Technology for Predicting Sediment Yields and Sources, US Department of Agriculture Publication ARS-S 40:33–45.

Rozos, D., H. D. Skilodimou, C. Loupasakis, and G. D. Bathrellos. 2013. Application of the revised universal soil loss equation model on landslide prevention. An example from N. Euboea (Evia) Island, Greece. *Environmental Earth Sciences* 70 (7):3255–3266.

Sinha, D., and V. U. Joshi. 2012. Application of Universal Soil Loss Equation (USLE) to recently reclaimed badlands along the Adula and Mahalungi Rivers, Pravara Basin, Maharashtra. *Journal of the Geological Society of India* 80 (3):341–350.

Telles, T.S., M. Guimaraes, and S.C.F. Dechen. 2011. The costs of soil erosion. *Revista Brasileira de Ciência do Solo* 35: 287-298. DOI: 10.1590/S0100-06832011000200001

USDA. 1972. National Engineering Handbook. Soil Conservation Service. US Department of Agriculture, Washington, DC, Sect. 3.

USDA. 2002. NRCS: State Oce of Michigan, Technical Guide to RUSLE Use in Michigan.

USDA SCS. 1979. United States Department of Agriculture - Soil Conservation Service. National Engineering Handbook, Sec. 4. Hydrology.

USDA. 2013. Science Documentation. RUSLE2. Washington DC: USDA.

USGS. 2019a. USGS 05559700 SENACHWINE CREEK AT CHILLICOTHE, IL. *National Water Information System: Web Interface*. https://waterdata.usgs.gov/nwis/inventory/?site_no=05559700&agency_cd=USG S (last accessed 18 November 2019).

USGS. 2019b. National Geospatial Program. *The National Map*. https://www.usgs.gov/core-science-systems/national-geospatial-program/national-map (last accessed 18 November 2019).

USGS. 2019c. EarthExplorer - Home. *EarthExplorer*. https://earthexplorer.usgs.gov/ (last accessed 18 November 2019).

Van der Knijff, J.M., Jones, R.J.A., and Montanarella, L. 2000. Soil Erosion Risk Assessment in Europe. https://www.preventionweb.net/files/1581_ereurnew2.pdf (last access: 21 November 2018).

Vanoni, V.A. 1975. Sediment deposition engineering. ASCE Manuals and Reports on Engineering Practices. 54.

Vente, J. D., J. Poesen, M. Arabkhedri, and G. Verstraeten. 2007. The sediment delivery problem revisited. *Progress in Physical Geography: Earth and Environment* 31 (2):155–178.

Wall, A. F., and W. D. Allmon. 2014. Soils of the Midwestern US. In *Fossils of the Midwestern US*, 57–83. Ithaca, NY: Paleontological Research Institution.

Walling, D. E. 1983. The sediment delivery problem. *Journal of Hydrology* 65 (1-3):209–237.

White, S. 2005. Sediment yield prediction and modelling. *Hydrological Processes* 19 (15):3053–3057.

White, W. P., A. Phillips, J. Beardsley, D. Devotta, and G. Pociask. 2008. *Senachwine Creek Watershed Assessment Report*. Springfield, IL: Illinois Department of Natural Resources.

Wilkinson, B. H., and B. J. McElroy. 2006. The impact of humans on continental erosion and sedimentation. *Geological Society of America Bulletin* 119 (1-2):140–156.

Wischmeier, W.H., D.D. Smith. 1978. Predicting rainfall erosion losses: a guide to conservation planning. *USDA Agriculture Handbook*. 537.

Young, A. 1994. *Land degradation in South Asia: its severity, causes, and effects upon the people*. Rome: Food and Agriculture Organization of the United Nations.

CURRICULUM VITA

NAME: Jonah Neal Liebman

ADDRESS: Department of Geography and Geosciences
200 E. Shipp Avenue
University of Louisville
Louisville, KY 40208

DOB: Louisville, Kentucky – July 4, 1994

EDUCATION
& TRAINING:

B.A., Environmental Earth Science
Washington University
2012-16

ArcGIS Certificate
2018

PROFESSIONAL SOCIETIES:

Kentucky Academy of Sciences
American Association of Geographers
Kentucky Association of Mapping Professionals
Olmstead Parks Conservancy